A Comparative Study on the Mechanical, Thermal, and Water Barrier Properties of PLA Nanocomposite Films Prepared with Bacterial Nanocellulose and Cellulose nanofibrils

Baraka Gitari,[a] Boon Peng Chang,[a] Manjusri Misra,[a,b,*] Alireza Navabi,[c] and Amar K. Mohanty [a,b,*]

Mechanical, thermal, and water barrier properties of poly(lactic acid) (PLA) film reinforced with cellulose nanofibrils (CNF) and bacterial nanocellulose (BNC) were studied and compared. The *in-situ* formation of sodium carbonate (Na_2CO_3) on the BNC surface may aid in reducing the interchain hydrogen bonding and agglomeration of BNC fibers. At optimum loading, both CNF/PLA and BNC/PLA nanocomposite films exhibited higher tensile strength and Young's modulus than the neat PLA without sacrificing its toughness. The BNC/PLA nanocomposite films displayed lower water vapor transmission rate (WVTR) as compared to neat PLA and CNF/PLA films at 0.5 and 1.0 wt%. BNC was found to induce imperfect crystal structures and exhibited higher overall crystallinity than neat PLA and CNF/PLA composites at 0.5 wt%. The BNC/PLA showed higher mechanical properties than CNF/PLA nanocomposites. Nanocellulose derived from plants and bacteria could provide promising solutions to develop high performance biobased-nanocomposites film for packaging application.

Keywords: Poly(lactic acid); Nanocomposite films; Bacterial nanocellulose; Mechanical properties

Contact information: a: Bioproducts Discovery and Development Centre (BDDC), Department of Plant Agriculture, Crop Science Building, University of Guelph, 50 Stone Road East, Guelph, N1G 2W1, Ontario, Canada; b: School of Engineering, Thornbrough Building, University of Guelph, 50 Stone Road East, Guelph, N1G 2W1, Ontario, Canada; c: Department of Plant Agriculture, Crop Science Building, University of Guelph, 50 Stone Road East, Guelph, N1G 2W1, Ontario, Canada;
**Corresponding authors: M. Misra, mmisra@uoguelph.ca; A. K. Mohanty, mohanty@uoguelph.ca*

INTRODUCTION

The plastic packaging industry consumes the largest market sector of plastic resins, and their products are widely used in food and beverage, pharmaceutical, and other consumer goods (Plastics Europe 2013; Dahlbo *et al.* 2018). Most of the plastic packaging materials in the form of bottles, film, sheets, *etc.* are used one time and disposed. The increasing use of these pre- and post-consumer plastic packaging wastes every year contributes to environmental pollution, which affects the ocean and wildlife ecosystems. This phenomenon has reached global concern, and developed countries including Canada, United State, Japan, Germany, France, and China have taken a leading role by implementing new rules and regulations to reduce the plastic bags consumption and waste. Biobased and biodegradable plastic (bioplastic) packaging materials have emerged as an important field of study and development that has the potential to replace non-degradable petroleum-based plastic for packaging applications. In recent years, sustainable bioplastics, *e.g.* poly(lactic acid) (PLA) synthesis from renewable biomass feedstocks, have been

studied as a potential alternative to petroleum-based plastics (Auras *et al.* 2003; Datta and Henry 2006). Although bioplastic packaging materials from starch-based materials and PLA are already commercially available in the market, the brittleness, poor barrier properties, low impact strength, lack of thermal stability, and high cost of PLA as compared to certain conventional plastics such as polyethylene (PE) and polystyrene (PS) has placed limits on its applications. These drawbacks can be addressed through proper modification of PLA with appropriate additives and processing technique. Auras *et al* (2003) reported that the mechanical and barrier properties of the two biaxially orientated PLA films are comparable to synthetic plastic films, PS, and polyethylene terephthalate (PET).

Blending of PLA with other thermally stable polymers, filler and fiber has been shown to enhance the properties of PLA (Wang *et al.* 1998; Kasuga *et al.* 2003; Huda *et al.* 2007; Lee *et al.* 2009a; Quero *et al.* 2009; Li *et al.* 2010; Tomé *et al.* 2011; Lee *et al.* 2012; Quero *et al.* 2012; Ma *et al.* 2013; Fortunati *et al*. 2015; Abdulkhani *et al*. 2014; Haafiz *et al*. 2013; Hubbe *et al.* 2017). Wang *et al.* (1998) studied the performance of PLA/poly(ε-caprolactone) (PCL) blends with triphenyl phosphite (TPP) as a coupling catalyst. They found that the elongation at break of the blends was increased significantly (approximately 560%) as compared to neat PLA. However, the tensile strength and elastic modulus decrease dramatically compared with neat PLA. Biodegradable blends from PLA and poly(*β*-hydroxybutyrate-co-*β*-hydroxyvalerate) (PHBV) also showed a significant increase in elongation at break (from 4% to 220%) as compared with neat PLA (Ma *et al.* 2013). Similarly, the tensile strength and flexural modulus were also found to be lower than neat PLA after blending with PHBV. Kasuga *et al.* (2003) used calcium carbonate (vaterite) as a reinforcement in PLA to develop biomaterials for synthetic bone plates. Significant improvements in modulus elasticity and bending strength were observed. However, these improvements come with an increase in porosity and a decrease in toughness. In summary, modification of PLA through co-polymer blending and fillers reinforcement usually increases some properties with some tradeoff in other properties.

Cellulose is one of the fastest growing emerging biomaterials. It is composed of D-glucose linked by *β*-1,4-glycosidic bonds. It is chemically versatile, biocompatible, hydrophilic, transparent, insoluble in water, and compostable (Auras *et al.* 2003; Gallegos *et al.* 2016). The incorporation of small amount of nano-size cellulose (nanocellulose) in polymer can boost the performance of the nanocomposites significantly. Nanocellulose can be extracted from plant and bacteria. A number of works have been conducted by several authors on the reinforcing effect of nanocellulose in polymer biocomposites (Lee *et al.* 2009a; Quero *et al.* 2009; Li *et al.* 2010; Tomé *et al.* 2011; Lee *et al.* 2012; Quero *et al.* 2012; Panaitescu *et al.* 2017), and a summary and thorough review of the use of these nanofibers in polymer have been discussed and reported by Lee *et al.* (2014).

Cellulose nanofiber (CNF)-reinforced PLA has been shown to have better mechanical properties over the neat PLA (Haafiz *et al*. 2013; Abdulkhani *et al*. 2014; Fortunati *et al*. 2015; Hubbe *et al.* 2017). However, unmodified nanocellulose is usually not well dispersed in hydrophobic polymers due to incompatibility with the polymer phase resulting in poor mechanical performance (McLean 1982; Poyraz 2018). The dispersion and interaction of the hydrophilic BNC and hydrophobic PLA can be achieved through surface modification and compatibilization (Lee *et al.* 2009a; Li *et al.* 2010). Li *et al.* 2010 developed PLA nanocomposites with grafted maleic anhydride (MA) bacteria nanocellulose (BNC) fiber. The grafted nanocomposites with MA and benzoyl peroxide showed better properties than the unmodified BNC/PLA nanocomposites due to the improved compatibility between the BNC fibers and PLA. Abdulkhani *et al.* (2014)

prepared CNF/PLA cast films and they found that the tensile modulus, tensile strength and elongation at break increased significantly with appropriate CNF loading (Abdulkhani *et al.* 2014). The water vapor permeability of the nanocomposites films was also comparable to the neat PLA film. A summary of some studies related to nanocellulose-reinforced PLA is presented in Table 1.

Plant-based cellulose has variable properties depending on its growth conditions, plant species, and location in the plant. Additionally, it requires extensive purification steps known as the kraft process to separate and purify cellulose fibers from lignin, hemicellulose, and other biopolymers (Wang *et al.* 1998; Tomé *et al.* 2011). BNC is a renewable extracellular nanocellulose produced by acetic acid bacteria in sugar-rich growth mediums (Jozala *et al*. 2016). It is a viable alternative to plant-based cellulose due to the fewer purification steps required and higher crystallinity (Segal *et al.* 1959; Chen *et al.* 2011). In addition, BNC outperforms current in use cellulose in the food industry and technology as effective hydrocolloid additive (da Gama and Dourado 2018).

Table 1. Some Mechanical Properties of Nanocellulose Fiber Reinforced PLA Nanocomposites and their Optimum Fiber Loading

Composite designation	Nanocellulose (wt%)	Processing Method	Young's Modulus (MPa)	Tensile Strength (MPa)	Elongation (%)	Ref.
PLA_3CNC	3	Solution Cast	1930	100.9	2.7	(Fortunati *et al*. 2015)
PLA/CNF 3	3	Solution Cast	1200	33.1	188.9	(Abdulkhani *et al*. 2014)
PLA-CNF5	5	Solution Cast	4150	15.75	60	(Haafiz *et al*. 2013)
BCG/MA-PLA	~15.5	Solution Cast	3000	46.85	1.4	(Quero *et al.* 2012)
PLA/ 0.5BCNF	0.5	Melt mixing and two-roll mill	3192	53.7	6.5	(Panaitescu *et al.* 2017)
BC-g-MA/PLA/ BPO	6.0	Solution Cast	2308	31.39	3.3	(Li *et al.* 2010)

This work aims to study and compare the mechanical, thermal, and water barrier performance of two different feedstock of nanocellulose, *i.e.* CNF and BNC reinforced PLA films. Different cellulose contents (0.5, 1.0, and 2.0 wt%) were incorporated into PLA through solution casting followed by compression molding. The synthesized BNC was characterized with X-ray diffraction (XRD), differential scanning calorimetry (DSC), and scanning electron microscopy (SEM).

EXPERIMENTAL

Materials and Methods

Bacterial broth preparation

A standard Hestrin Schramm (HS) growth medium was prepared (Hestrin *et al.* 1947) in 24 Erlenmeyer flasks. 100 mL of the HS medium was added to in each flask. All flasks were capped with aluminum foil and sterilized in an autoclave. The aluminum caps

remained on the Erlenmeyer flasks throughout the seeding and growing process to limit oxygen concentrations available to *Komagateibacter xylinus* and to minimize the risk of contamination.

Growing process

The contents of the *Komagateibacter xylinus* ATCC 53524 glass vile (American Type Culture Collection, Manassas, VA, USA) were transferred to a 5 mL solution of the growth medium. This inoculation was incubated at room temperature for a week. Next, 0.1 mL of this solution was transferred to each of the Erlenmeyer flasks. The flasks were incubated at 30 °C for 14 days. At the end of the growth cycle, the pellicles were collected, and the growth medium was discarded.

Cellulose processing and purification

A standard kitchen blender was used to blend the pellicles in 1 L of deionized (DI) water three times for 20 second intervals. Once blended, ~4 g NaOH (0.1 mol/L) was added into the mixtures. This mixture was then heated and stirred for 10 min on a hot plate at 150 °C. The mixture (25 mL) was poured into 50 mL plastic falcon tubes and centrifuged at 8000 rpm for 10 min with a Thermo Scientific Sorvall ST-8 Centrifuge (Thermo Scientific, Mississauga, Canada). The supernatant was decanted, and the precipitate (nanocellulose) was kept. The hydrolysis and centrifuging process were repeated three times. Finally, the precipitate was stored in a refrigerator at 4 °C. The detail purification process of the bacteria nanocellulose (BNC) fiber are presented in Fig. 1. Approximately 1 mL of acetone was added to each tube to prevent the growth of fungi during long term storage.

Hydrated softwood purified cellulose nanofibrils (CNF) were supplied by the University of Maine Nanocellulose Facility (Orono, ME, USA). All nanocellulose samples were dried for 3 days on a Petri dish in the fume hood before cryogrinding. In order to directly compare the properties of CNF/PLA and BNC/PLA nanocomposite films, all fibers used in this study were not surface treated.

PLA nanocomposite films preparation

PLA films fabricated by compression moulding after solution casting have been shown to have higher mechanical properties (Rhim *et al.* 2006). The neat PLA and its nanocomposite films (0.5, 1.0, and 2.0 wt%) were prepared with solution casting followed by compression molding. The nanocellulose was cryoground to minimize broad size distribution and to obtain a finer and uniform size of BNC. Then, the cellulose was dispersed overnight in 250 mL of acetone. Approximately 20 g of film grade PLA 4043D pellets (NatureWorks, Minnetonka, MN, USA) were dissolved in 400 mL of chloroform (Sigma Aldrich, Oakville, Canada) and stirred overnight. After each solution was mixed overnight, the nanocellulose was added to the chloroform mixture for another 4 h. The obtained final solution was then poured into a standard anti-stick baking pan with dimensions of 450 (l) × 275 (w) × 30 (t) mm. The solvents were evaporated for 24 h in a fume hood.

The prepared films were placed between metal plates covered with a Teflon film to prevent sticking. All films were degassed by applying and releasing pressure three times to ensure the films were free from air bubbles. The films were compressed using a Carver hydraulic press (Carver, Inc., Wabash, IN, USA) at 180 °C and ~40 MPa for 2 min. The samples were then cooled down while still under pressure for 6 min.

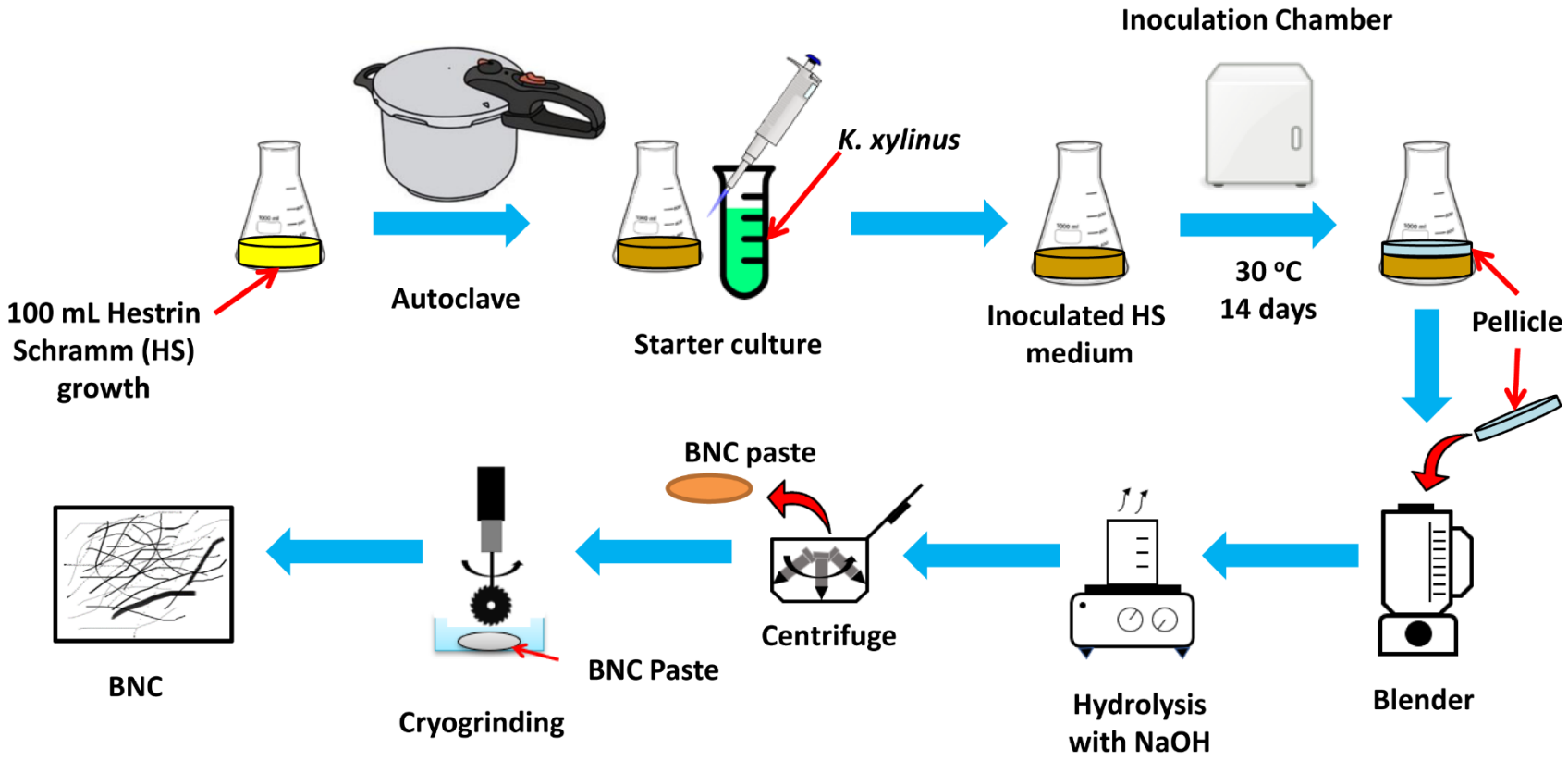

Fig. 1. Synthesis and preparation process of bacteria nanocellulose (BNC)

The films were removed from the mold and cut into dimensions of 150 (l) × 10 (w) × 0.1 (t) mm and 50 (l) × 50 (w) × 0.1 (t) mm for tensile testing and water barrier testing, respectively. All films were stored at 25 °C at 50% RH before testing.

Characterization

X-ray diffraction

The cryoground nanocellulose samples were imaged with a Bruker XRD D8 Discover with Davinci design diffractometer (Billerica, MA, USA). A cobalt source was used (λ_{avg} = 1.79026 Å) to image the sample between 8° and 45°. Two measurements were taken from a CNF, unwashed BNC, and BNC washed with 1 L DI over a Hirsh Funnel. The amorphous peak was set to 24.1°, and crystal information file (CIF) files were used to define the crystalline peaks. The CIF was based on the March Dollase preferred orientation of the Miller index 100 and 110 directions (Dollase 1986).

Fourier transform infrared (FT-IR) spectroscopy analysis

The functional groups and bonding present on the BNC surfaces with and without sodium carbonate were carried out using Thermo Scientific, Nicolet 6700 Fourier transform infrared spectroscopy (FTIR) from Thermo Fisher Scientific, Waltham, Massachusetts, America. All the samples were scan in the range of 4000 to 600 cm^{-1} wave number with a 4 cm^{-1} resolution and 64 scans.

Mechanical testing

The tensile test of the PLA nanocomposite films was performed based on ASTM D882-18 using an Instron Universal Testing Machine (UTM) model 3382 (Norwood, MA) with video extensometer. Each film was clamped into the tensile grips with a 100 mm gauge length, and a 50 mm/min crosshead speed was used. Six films for each sample were tested and the means and standard deviation were reported.

Differential scanning calorimetry (DSC)

The thermal analysis of the PLA films was conducted in a DSC Q200 (TA Instruments, Grimsby, Ontario, Canada). The procedure was as follows: set to equilibrate at 30 °C then ramp 10 °C/min to 200 °C where it was isothermal for approximately 2 min. It was then cooled from 200 °C to 30 °C at 10 °C/min and was isothermal for 2 min. The third cycle was ramped at 10 °C/min to 200 °C. The first heating cycle of the DSC thermograms was used to determine melting temperature (T_m) and crystallization temperature (T_c) as to not erase thermal history when calculating crystallinity. The DSC thermograms of the second heating cycle (third cycle) were used to determine glass transition temperature (T_g).

The degree of crystallinity (X_c) values of all samples were determined from the first heating of the DSC thermograms. The relationship between the area under the curve of the first melting peak of the nanocellulose/PLA composites and 100% crystalline PLA was used to calculate the crystallinity of each sample. The X_c calculation is shown in Eq. 1 below,

$$X_c = \frac{\Delta H_m - \Delta H_{cc}}{\Delta H_{100}(1 - w_f)} \times 100\% \quad (1)$$

where ΔH_m is the area under the curve (enthalpy) of the melting peak, ΔH_{cc} is the area under the curve of the cold crystallization peak, ΔH_{100} is the melt enthalpy of 100% crystalline PLA, which was found to be 93.0 J/g (Nam *et al.* 2003), and w_f is the weight

fraction of the nanocellulose loadings.

Water barrier testing

Gravimetric testing was used to determine the barrier properties of each biocomposite film. An Endurance C340 environmental chamber (Associated Environmental Systems, Acton, MA, USA) was set to 37.8 °C and a 90% RH. Approximately 20 to 30 dried silica beads were placed into 3 light metal cups with a 40 mm diameter at the rim and a depth of 50 mm. Each cup was sealed with the prepared film pieces (50 × 50 × 0.1 mm) using epoxy glue. The initial weight of each metal cup with dried silica and glued film was measured as an initial reading. Then the cups were placed into the environmental chamber. The weight of the cups was measured every 20 min for the first 2 h and every hour for the subsequent 4 h. Finally, each cup was measured at 24 and 48 h after the first measurement to ensure that the weight of the cups remained consistent. Consistent weight over time indicates that the silica beads and film were saturated with DI water and that the experiment was complete. The slope of time (min) *vs.* weight (g) for the first 6 points was the water vapor permeability value after conversion to $g \cdot mL/m^2 \cdot day$.

Thermogravimetric Analysis (TGA)

A TGA Q500 was used (TA Instruments, New Castle, Delaware, America). Approximately 5 mg of dry film sample were placed onto the platinum pan and heated at a rate of 10 °C /min from room temperature to 700 °C.

Statistical analysis

The statistical analysis of the performance of the PLA films was carried out using SAS University Edition version 9.4 (Cary, NC, USA). The experimental design was completely randomized. Each experimental unit was a piece of tensile film. There were 5 experimental units for tensile test (Young's modulus, tensile strength, and elongation at break), 3 replicates for water vapor transmission rate (WVTR), and 2 for differential scanning calorimetry (DSC). All type I error rates were set at (P = 0.05) unless otherwise stated. Nanocellulose sources, BNC and softwood CNF, and loading (0.5, 1.0, and 2.0 wt%) were independent variables, while Young's modulus, tensile strength, elongation at break, WVTR, and crystallization percent calculated with DSC thermograms were considered dependent variables. Comparative tests were conducted between CNF/PLA and BNC/PLA composites for tensile strength. Furthermore, contrasting tests were also run between 0.5 and 1 wt% CNF/PLA and BNC/PLA nanocomposites film for WVTR and modulus.

RESULTS AND DISCUSSION

X-Ray Diffraction (XRD)

The X-ray diffraction spectra of CNF and BNC are presented in Fig. 2 (a). The CNF showed customary features distinct to crystalline cellulose ($I_{1\,-1\,0}$), ($I_{1\,1\,0}$), (I_{AM}), (I_{002}), and (I_{400}), which indicated that the sample was crystalline cellulose (Park *et al.* 2010; Luo and Wang 2017). Using the March Dollase method (Dollase 1986), the crystallinity of CNF was calculated to be 78% and 80% for the first and second measurements, respectively. These values are similar to those reported by Chen *et al.* (2011), who employed the Segal

method (Segal *et al.* 1959) and found the crystallinity of softwood CNF to be 80.2% ± 4.2%. The crystallinity of the washed BNC sample using the same method was calculated to be 79% and 90% for the first and second measurements, respectively. Bacterial nanocellulose was reported to have higher crystallinity than CNF (Poyraz 2018). However, the unwashed BNC appears to be in an amorphous phase as shown in Fig. 2 (b). This may be due to the presence of other functional groups on the BNC surfaces and hence very little crystalline peaks were observed in the BNC characteristic peaks of ($I_{1\ -1\ 0}$), ($I_{1\ 1\ 0}$), (I_{002}), and (I_{400}). Furthermore, the peak pattern is consistent with sodium carbonate (Na_2CO_3), suggesting that there were substantial amounts of Na_2CO_3 on the sample. To purify the BNC, 0.1 N NaOH was used (Eq. 2). In addition, when blending and mixing the pellicle which has trapped CO_2 from cellular respiration of the bacteria (Jozala *et al*. 2016) and in the presence of air containing, carbon dioxide (CO_2) could mix into the solution (Eq. 3). The product of the previous two reactions likely formed Na_2CO_3 (Eq. 4). However, the amount of Na_2CO_3 produced is difficult to control as it is formed in-situ during fiber processing and from respiration of the bacteria. The CO_2 has been shown to dissolve in water from air and form carbonic acid in soil and natural waters, lowering the pH of the respective medium (McLean 1982).

$$H_2O + NaOH_{(aq)} \rightarrow Na^+ + OH^- + H_2O \quad (2)$$

$$CO_2 + H_2O \rightarrow H_2CO_3 \rightleftharpoons 2H^+ + CO_3^- \quad (3)$$

$$2Na^+ + CO_3^- \rightarrow Na_2CO_3 \quad (4)$$

The formation of carbonate (CO_3) as a result of NaOH treatment decreases hydrogen bonding between fibers of nanocellulose, which could favorably affect the dispersion of nanocellulose in its respective matrix (Zhang *et al.* 2015; He *et al.* 2016). A proposed schematic drawing of BNC with and without the presence of CO_3 is presented in Fig. 3 parts (a) and (b), respectively. CO_3 could inhibit the inter-chains hydrogen bonding between BNC. He *et al.* (2016) synthesized precipitate calcium carbonate hybrid CNF and used to fabricate paper nanocomposites. The produced CNF/paper had a better dispersion and tensile strength due to the presence of calcium carbonate as compared to unmodified CNF/paper composites and conventional paper. This was attributed to the deposition of carbonate on the CNF, which decreases hydrogen bonding between fibers and results in a more dispersed network of CNF in the paper (He *et al.* 2016). Zhang *et al.* (2015) conducted a study to determine the effects that milling time, ball mill size, and alkaline pre-treatment with Na_2CO_3 has on the morphology of nanocellulose fibers. The Na_2CO_3 in alkaline conditions in conjunction with ball-milling procedure weakens the hydrogen bonds in between cellulose nanofibrils (Zhang *et al.* 2015).

Fourier Transform Infrared (FT-IR) Characterization

The FTIR spectra of the BNC with and without Na_2CO_3 are shown in Fig. 4. The BNC with Na_2CO_3 was prepared according to the cellulose processing method discussed in the methodology section above. For the BNC without Na_2CO_3 sample, the BNC was filtered and washed several times with distilled water to remove the Na_2CO_3 from the surface.

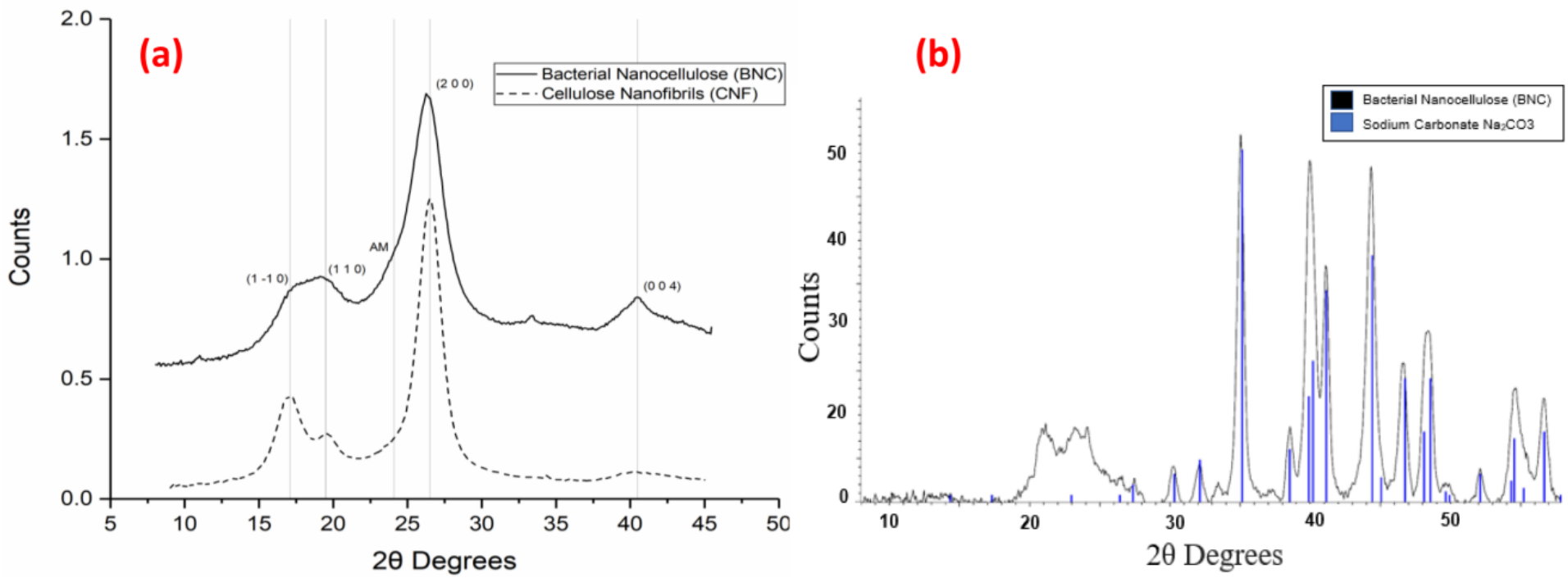

Fig. 2. (a) XRD curves of purified BNC and softwood CNF and (b) XRD curves of streamlined process BNC and sodium carbonate

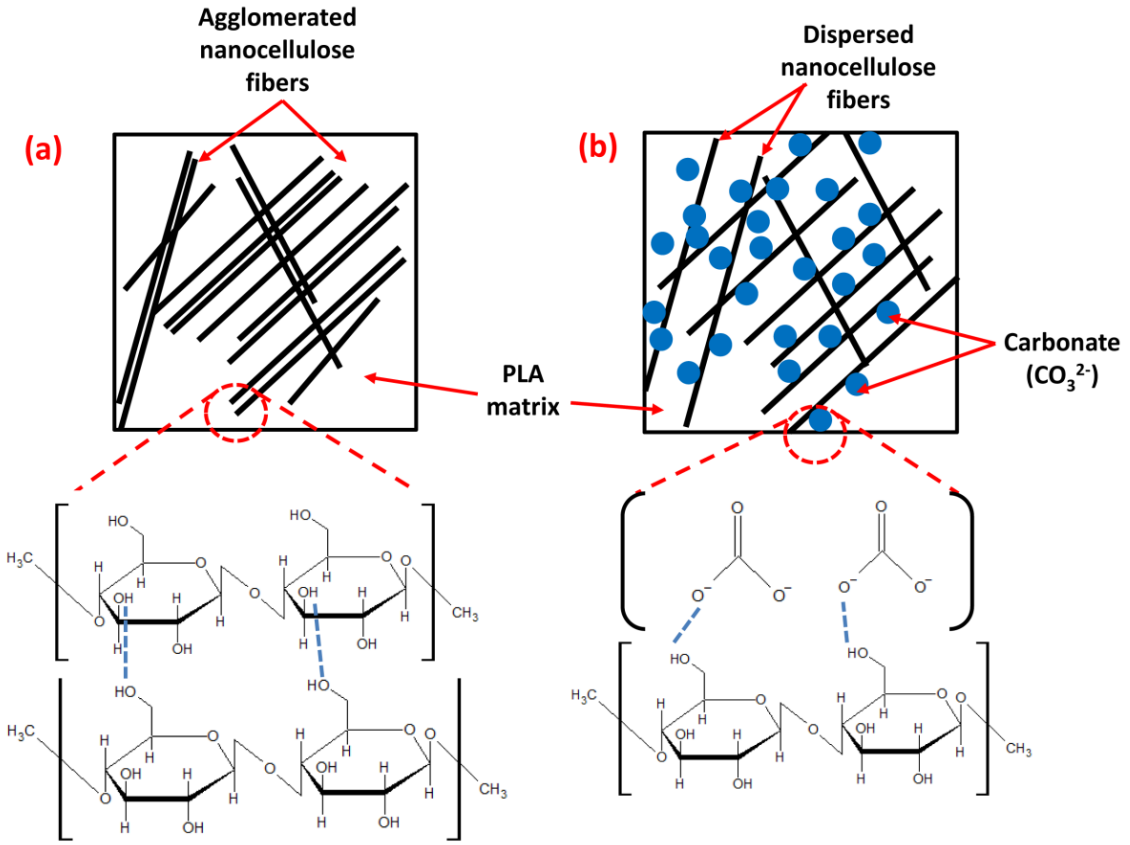

Fig. 3. Proposed interaction of CO_3^{2-} inhibiting interchain hydrogen bonding left (a) without CO_3^{2} and right (b) with CO_3^{2}

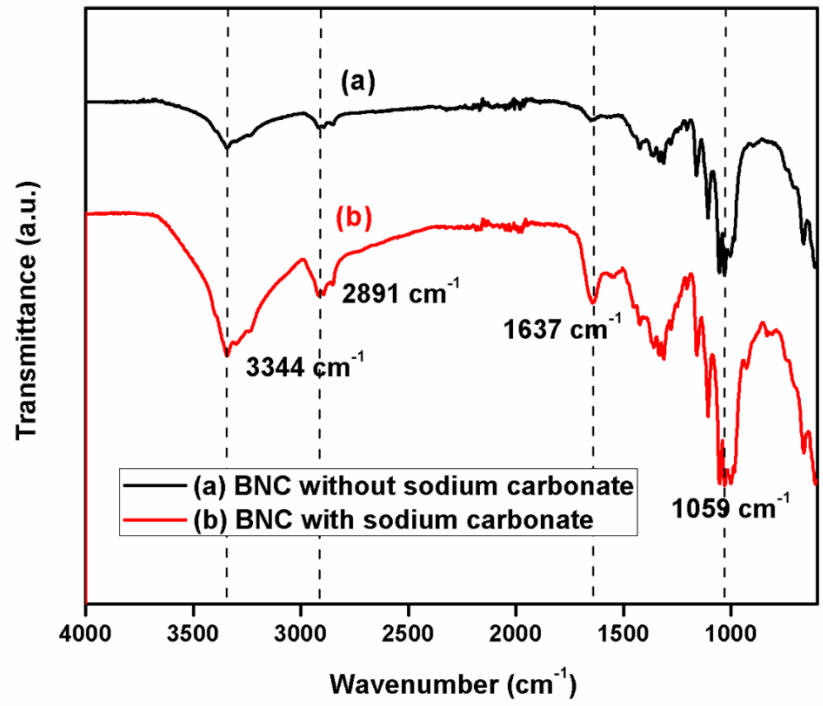

Fig. 4. FTIR analysis of the bacterial nanocellulose with and without the presence of sodium carbonate

From the FTIR spectra, the band at 3344 cm^{-1} corresponds to the intermolecular hydrogen bonded O-H stretching of cellulose I (Moharram and Mahmoud 2008). The band around 2891 cm^{-1} is due to the CH_2 stretching, while the broad band at 1640 to 1650 cm^{-1} can be attributed to the H-O-H bending vibration of absorbed water molecules (Mohammadkazemi 2017). The peaks in the range of 1050 to 1059 cm^{-1} correspond to the ether C-O-C and C-OH stretching vibrations (Gea 2010).

It was found that there is no obvious shifting of the peak and formation of new peak between the BNC with and without Na_2CO_3. However, the intensity of the hydroxyl band was broadened in the spectrum of BNC with Na_2CO_3. This may be due to the presence of intermolecular hydrogen bonding between hydroxyl groups of BNCs and CO_3^{2-} ions as discussed earlier (Fig. 3).

Mechanical Properties

The effects of CNF and BNC in PLA films on the tensile properties are shown in Fig. 5 (a) and (b). Both nanocomposite films showed higher Young's modulus and tensile strength than the neat PLA. Fibers and fillers usually decrease chain mobility in their respective matrix. This leads to an increase in Young's modulus and tensile strength and a decrease in elongation (Mathew *et al.* 2006; Jonoobi *et al.* 2010). For both CNF/PLA and BNC/PLA nanocomposites, the Young's modulus increased with increased fiber loadings. The modulus of 0.5, 1.0, and 2.0 wt% CNF/PLA nanocomposites increased from 2539 MPa, 3075 MPa, and 3189 MPa, respectively. On the other hand, the modulus of 0.5, 1.0, and 2.0 wt% of BNC/PLA nanocomposites were 3400 MPa, 3750 MPa, and 3672 MPa, respectively. The hydrogen bonds between PLA and the natural nanocellulose fibers determine its mechanical strength (Nakagaito *et al.* 2009; Tee *et al.* 2013). Auad *et al.* (2008) reinforced polyurethanes (PU) with 1.0 wt% of nanocellulose and found that PU with nanocellulose increases tensile strength and Young's modulus over neat PU. They attributed the enhancement to the presence of stiff randomly orientated fibers, which additionally decrease the chain mobility of the PU. Similar mechanisms of action have been found in a number of nanocellulose/PLA nanocomposites as well (Lee *et al.* 2009a; Lee *et al.* 2009b; Quero *et al.* 2009; Li *et al.* 2010; Tomé *et al.* 2011; Lee *et al.* 2012; Quero *et al.* 2012).

The tensile strength of the CNF/PLA nanocomposites increased from 36.7 MPa (0.5 wt%) to 44.2 MPa (1.0 wt%) then decreased to 37.2 MPa for the 2.0 wt% fiber loading. For the BNC/PLA, the tensile strength of the 0.5 and 1.0 wt% were 49.9 MPa and 48.7 MPa, respectively. The tensile strength of the BNC/PLA was decreased at 2.0 wt% loading of BNC. Increasing nanocellulose loadings increases the chance that there are fibers throughout the PLA matrix, which could increase the strength; however, increasing loadings also increases agglomerations (Yeh *et al.* 2010; Shih *et al.* 2011). Qu *et al.* (2010) observed a decrease in tensile strength of BNC/PLA films composites where the fiber loading was greater than 3 wt%.

Neat PLA had an elongation at break at 1.9%. For 0.5 wt% of both CNF and BNC loading in PLA, the films showed similar elongation at break to neat PLA. At 1.0 and 2.0 wt%, the elongation at break of both nanocomposites films showed decreasing trend in elongation. Nanocomposites with 2.0 wt% had lower elongation % at break than the neat PLA. Similarly, the tensile toughness of BNC/PLA decreased with the increasing content of BNC (Fig. 5b). In comparison, the 2.0 wt% CNF/PLA decreased in elongation but to a lesser extent.

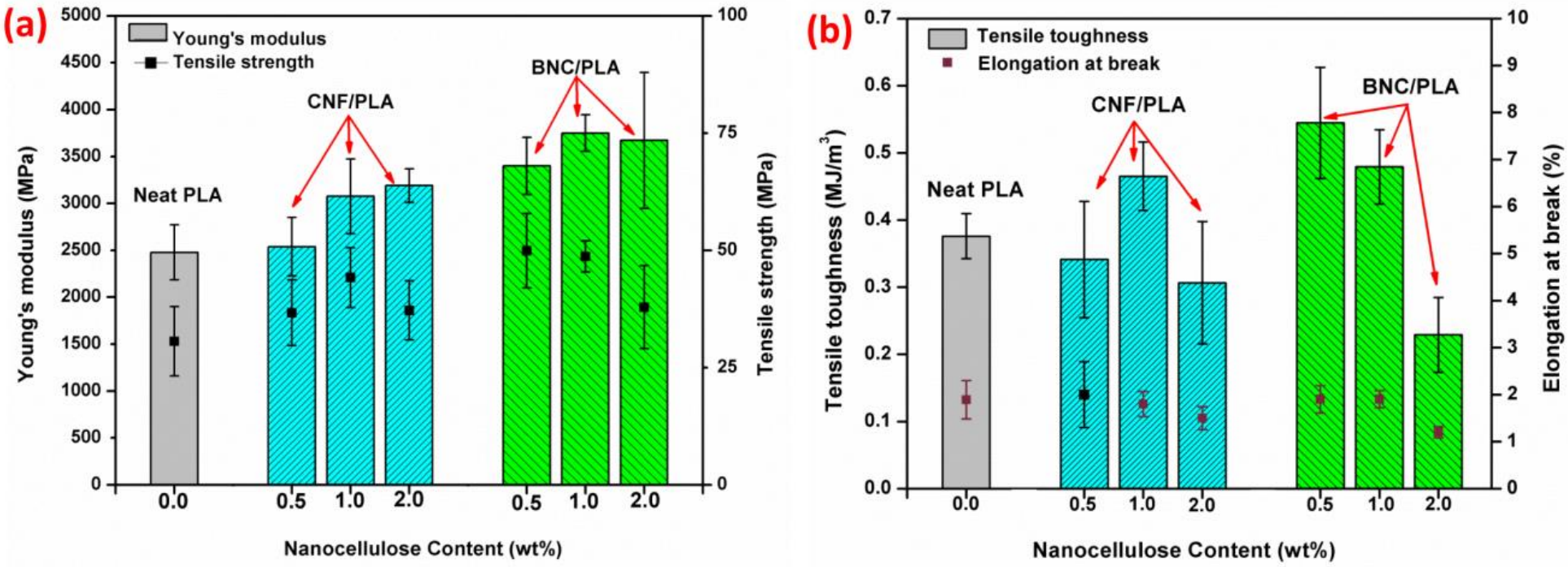

Fig. 5. Tensile properties comparison for neat PLA, CNF/PLA and BNC/PLA nanocomposites. (a) Young's modulus and tensile strength and (b) tensile toughness and elongation at break

The agglomerations of the cellulose fiber are likely to form at higher content, which results in a decrease in mechanical properties, *e.g.*, elongation at break (Abdulkhani *et al.* 2014; Yang *et al.* 2015). The formation of agglomerations of nanocellulose in the PLA matrix would explain why the elongation decreased from 1.0 to 2.0 wt% loadings.
According to the Cox-Krenchel equation, compatibilization between the polymer and reinforcing fiber as well as the modulus of the fiber itself affect the mechanical properties of the resultant composite (Cox 1952; Krenchel 1964). At each respective loading of nanocellulose fibers, the BNC/PLA composites had a higher tensile strength and modulus than the CNF/PLA nanocomposites. This can be due to the higher crystallinity of BNC as compared to CNF (Segal *et al.* 1959; Chen *et al.* 2011). This corresponds to the XRD results discussed earlier. The more ordered structure of BNC in comparison to CNF might yield greater mechanical properties of the fibers and hence the nanocomposites. Furthermore, CNF fibers easily agglomerate in the PLA matrix. On the other hand, the BNC was able to effectively disperse in a PLA solution because the NaOH solvent residues were not removed completely from the BNC. The fibers may have better interaction and distribution with PLA due to the presence of Na_2CO_3 on the surface as evidence in XRD results. Therefore, the mechanical performance of the BNC/PLA was higher than CNF/PLA nanocomposites. The 0.5 wt% and 1.0 wt% of CNF/PLA appears to be the ideal balance in this set of nanocomposites. A similar trend was observed with BNC/PLA nanocomposites. The compatibility between the PLA and BNC was likely to be highest at the 0.5 wt% and 1.0 wt% of BNC, as can be seen in higher strength and modulus without sacrificing the toughness as compared to neat PLA. At 2.0 wt% loading, the tensile strength of both CNF and BNC/PLA nanocomposite films showed downward trend due to the dominance of fiber agglomeration.

Differential Scanning Calorimetry (DSC)

Figure 6 shows the DSC heating curves for CNF/PLA and BNC/PLA nanocomposite films, respectively, compared with neat PLA. Table 2 shows the summary of DSC data. For the CNF/PLA nanocomposites, the T_g peaks are approximately 58 °C regardless of the CNF content. In comparison to BNC/PLA, the T_g of BNC/PLA nanocomposites increased with increasing cellulose wt% loadings. The 2.0 wt% BNC/PLA film composite had a similar T_g to the CNF/PLA composites. An increase in T_g is associated with decreased chain mobility of the PLA nanocomposites. The higher chain mobility of BNC/PLA as compared to CNF/PLA nanocomposite films might be due to the Na_2CO_3 on the BNC surfaces which give better flexibility.

The second exothermic peak observed is the cold crystallization peak (T_{cc}). The cold crystallization temperature is the temperature at which the newly mobile polymer chains arrange themselves into an ordered lattice. The peak produced corresponds to exothermal heat flow with respect to the polymer (Reading *et al.* 1994). Some fillers or fibers may act as nucleating agents through heterogeneous crystallization by generating sites for spherulite formation (Pei *et al.* 2010; Shi *et al.* 2015). As shown in Table 2, the T_{cc} of the BNC/PLA films occurs at a lower temperature than the neat PLA and CNF/PLA films. This shows the nucleating effect of the BNC which accelerates the crystallization of PLA (Panaitescu *et al.* 2017). Furthermore, the better distribution of BNC in the PLA as compared to CNF could results in more spherulite sites that promote heterogeneous crystallization.

The melting temperature (T_m) of PLA increased slightly after the addition of both CNF and BNC. There was a second endotherm melting peak adjacent to the T_{cc} peak in the 0.5 wt% BNC/PLA composite due to the incomplete crystalline structure forming (β-crystals). This peak seemed to shift to the right and became a shoulder for the original melting peak (α-crystal) in the 1.0 wt% BNC/PLA. The merging of the two peaks was observed at 2.0 wt% BNC/PLA nanocomposite. This most likely involves the amount of β-crystals that form upon crystallization. These are known to be the melting of imperfect and non-ordered crystallite structure due to the presence of nanocellulose, which have lower melting points and a higher chain mobility than the more commonly observed perfect α-crystals (Su *et al.* 2009; Mustapa and Shanks 2014). In addition, the presence of β-crystals structures aligns with the lower T_g of BNC/PLA in comparison to CNF/PLA (Puiggali *et al.* 2000). The double melting peaks were also observed in literature (Su *et al*. 2009; Shi *et al*. 2010). Shi *et al* observed double melting peaks in PLA thermograms with the addition of bamboo fibers.

The overall crystallinity was calculated and presented in Table 2. It was observed that the addition of both BNC and CNF (excluding 0.5 wt% CNF/PLA) increased the overall crystallinity of the PLA. This is similar to findings from Ten *et al.* in which loadings of nanocellulose whiskers (CNW) increased the crystallization of the Poly(3-hydroxybutyric acid-co-3-hydroxyvaleric acid) (PHBV) matrix (Ten *et al*. 2012). The growth of imperfect crystal structures (β-crystals) was observed in the BNC/PLA films. Although the growth of the perfect crystal structure (α-crystals) was interrupted, the total degree of crystallinity of the BNC/PLA films was higher than the CNF/PLA and neat PLA films for the 0.5 wt% nanocomposites. Total degree of crystallinity was found to be comparable for both CNF/PLA and BNC/PLA at 1.0 and 2.0 wt% nanocellulose content. Ghalia and Dahman (2017) reported a similar finding where the degree of crystallinity of PLA/polyethylene glycol (PEG) composites increases with the presence of BNC.

Table 2. DSC Data of Neat PLA, BNC/PLA, and CNF/PLA Nanocomposite Films

Nanocellulose Content/PLA (wt%)	Glass Transition Temperature (T_g)	Cold Crystallization Temperature (T_{cc})	Melting Temperature (T_m)	Total Degree of Crystallinity (%)
Neat PLA	53.16 ± 0.57	95.30 ± 2.77	142.39 ± 0.03	4.35 ± 1.16
0.5 CNF	58.11 ± 0.07	115.94 ± 1.83	146.18 ± 0.22	1.16 ± 0.18
1.0 CNF	58.17 ± 1.73	104.13 ± 0.44	145.51 ± 1.37	5.10 ± 1.31
2.0 CNF	58.81 ± 0.81	107.63 ± 0.41	145.10 ± 0.25	5.63 ± 1.19
0.5 BNC	51.25 ± 0.22	92.09 ± 0.10	148.70 ± 0.48	4.62 ± 0.27
1.0 BNC	54.70 ± 1.73	92.28 ± 3.73	147.61 ± 2.15	4.90 ± 0.95
2.0 BNC	58.81 ± 0.81	89.71 ± 1.26	146.07 ± 2.77	6.26 ± 0.931

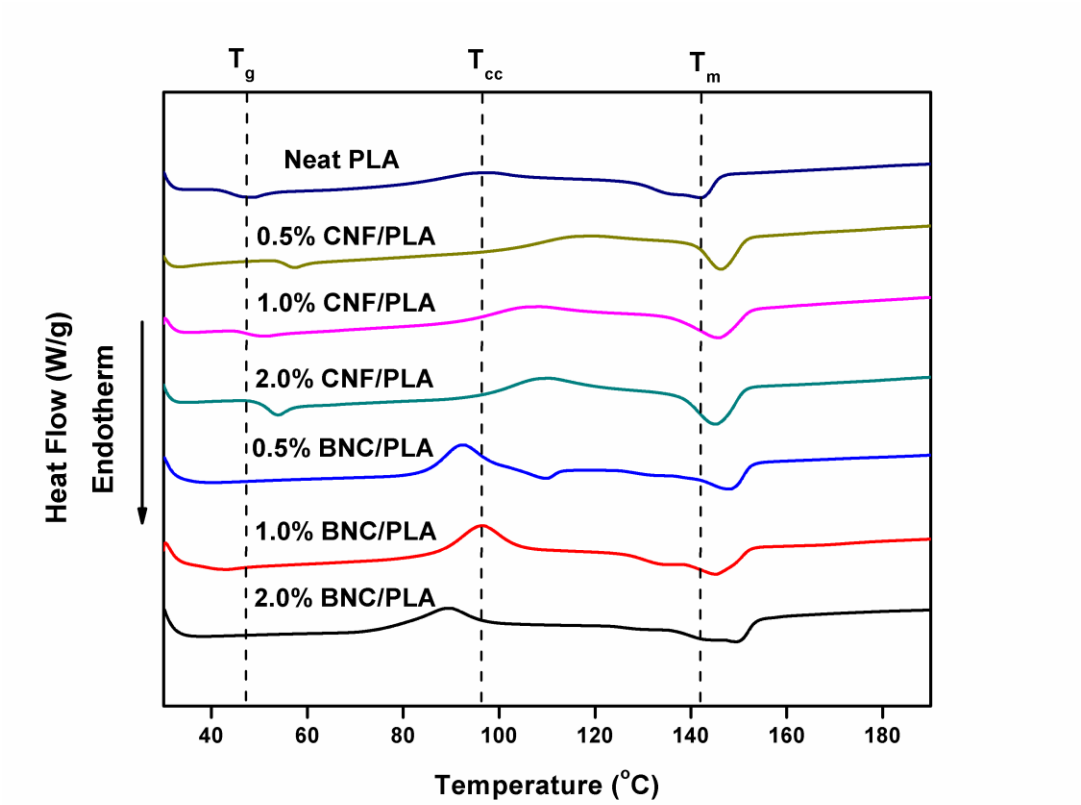

Fig. 6. DSC first heating curves of neat PLA, CNF/PLA, and BNC/PLA nanocomposite films

Water Vapor Transmission Rate (WVTR)

Water vapor transmission rate (WVTR) measures the resistance of a material to water vapor permeation, which is important for a packaging film. A low WVTR is a particularly desirable property for food packaging and biomedical applications. Figure 7 presents the WVTR of neat PLA, CNF/PLA, and BNC/PLA as a function of nanocellulose content at 37.8 °C and 90% humidity. Neat PLA was tested to have a WVTR of approximately 647 g·mL/m^2·day. Fibers in a polymer matrix can generate a longer path for gasses to travel before they penetrate the composite. This longer path is referred to as a tortuous path and is expected to be the mechanism in which fibers increase water or gas barrier properties (Gacitua *et al.* 2005). Additionally, the fiber loading should be controlled to optimum levels as a high content of fiber/filler can deteriorate the barrier properties. The WVTR for the BNC/PLA nanocomposite films decreased with an increasing amount of nanocellulose. However, the WVTR for 2.0 wt% BNC/PLA increased drastically. It is more difficult for water vapor to travel through crystalline regions in comparison to amorphous regions of a polymer (Salame 1986) and BNC is more crystalline than CNF. Furthermore, dispersed fibers generate a tortuous path, decreasing WVTR. With the high loadings of BNC, the fibers start to form agglomerations (Gacitua *et al.* 2005; Aulin *et al.* 2012) and may aid in the transport of water vapor across the matrix.

In the case of CNF/PLA, the WVTR increased linearly with an increase of the CNF content in the PLA matrix. The increase in WVTR is due to the gradual increase in agglomerations as the content of CNF in the PLA matrix increases. In comparison to the neat PLA and its nanocomposites, it is shown that the WVTR of BNC/PLA at 0.5 and 1.0 wt% is better.

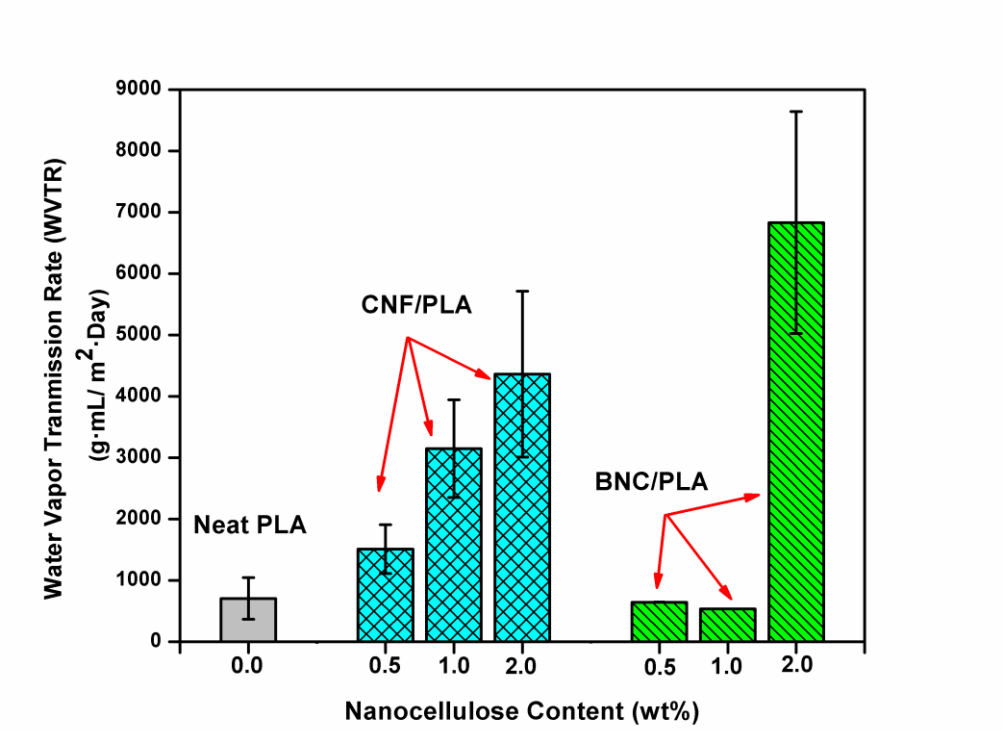

Fig. 7. Water vapor transmission rate of neat PLA (left bar), CNF/PLA (middle 3 bars), and BNC/PLA (right 3 bars) as a function of nanocellulose content at 37.8 °C and 90% RH

Table 3. Contrast Tests of Tensile Strength, Modulus, and WVTR between BNC/PLA and CNF/PLA Nanocomposites

Test	Selected formulations (wt%)	NumDF	DenDF	Alpha, α	nc	f_{crit}	Power
Tensile Strength	0.5, 1, and 2	1	28	0.05	8.4875	4.1960	0.8029
WVTR	0.5 and 1	1	14	0.05	15.8676	4.6001	0.9589
Modulus	0.5 and 1	1	28	0.05	11.0899	4.1960	0.8951

Statistical Analysis

Table 3 shows three different contrast tests that compare the performance of BNC/PLA with CNF/PLA nanocomposites of the same wt% loading. A "nc" value that is larger than a "f_{crit}" value for a test indicates that the performance of the BNC/PLA with same formulations used are different than CNF/PLA with statistical significance; tensile strength 8.4875 (nc) > 4.1960 (f_{crit}). The WVTR row shows the results of a contrast test between the WVTR of BNC/PLA and CNF/PLA nanocomposite films at the same content of the fiber (0.5 wt% and 1.0 wt%). The nc value of 15.8676 is greater than the f_{crit} value of 4.6001. This indicates that the WVTR of 0.5 wt% and 1.0 wt% of BNC/PLA are different in comparison to 0.5 wt% and 1.0 wt% of CNF/PLA. The results corresponded with the WVTR data (Fig. 7) where BNC/PLA films had a lower WVTR value in comparison to CNF/PLA nanocomposites at 0.5 wt% and 1.0 wt%.

The 2.0 wt% of BNC/PLA composites did not perform better than 2.0 wt% CNF/PLA. This may be due to agglomerates of nanocellulose that form at greater than 1.0 wt% loadings of nanocellulose in PLA as discussed before. A power of greater than 0.8 or greater than 80% is considered satisfactory. Power is the probability of rejecting the null hypothesis when it is false (Bowley 2015). In this case, the null hypothesis is that BNC/PLA and CNF/PLA nanocomposites have the same performance in each respective test. In general, the contrast test concluded that the BNC/PLA films showed better performance with statistical significance compared with CNF/PLA films in term of mechanical properties and WVTR.

Thermal Stability

The thermal stability of neat PLA and its nanocomposite films were investigated by thermogravimetric analysis (TGA), and the degradation curves are presented in Fig. 8a. The PLA exhibited two steps of weight loss as temperature increased. The first drop in weight observed, starting at about 100 °C, is due to the evaporation of absorbed water. The second weight decrease observed at 250 °C is due to the degradation of PLA chains (Liu *et al.* 2010; Petinakis *et al.* 2010). After the incorporation of CNF into PLA, the decomposition temperature increased. However, similar degradation temperature was observed. The improvement on the initial degradation of PLA with the presence of CNF may be due to CNF network stabilizing the PLA matrix with hydrogen bonds (Blaker *et al.* 2011; Jonoobi *et al.* 2012). In contrast, BNC/PLA nanocomposites exhibited only single step degradation around 350 °C except for 2.0 wt% BNC/PLA (Fig. 8b). This was consistent with the results from Panaitescu *et al.* (2017), in which only single step degradation is observed for the PLA with incorporation of BNC. The major degradation involves a consolidation of depolymerization, dehydration, and decomposition of the cyclic structures of the cellulose (Amin *et al.* 2014). The details of the TGA data are shown in Table 4. At a weight loss of 5.0%, the PLA with 0.5 wt% of BNC content exhibited higher thermal stability than other PLA formulations. However, the degradation temperature of BNC/PLA nanocomposite films decreased with increasing BNC content. The more finely dispersed BNC is more susceptible to hydrolysis at higher temperatures and releases smaller compounds (CH_4, C_2H_4, H_2O, and CH_2O), which in turn promote the decomposition of the PLA chain (Liu *et al.* 2010; Petinakis *et al.* 2010). A similar phenomenon is observed when starch and wood fibers are incorporated into PLA, and the presence of these molecules is confirmed with TGA-FTIR analysis (Liu *et al.* 2010; Petinakis *et al.* 2010).

The CNF/PLA composites had a comparable thermal stability to neat PLA but degraded at slightly higher temperatures, while BNC/PLA nanocomposites did not exhibit significant weight loss before 250 °C but underwent degradation at lower temperatures than neat PLA and CNF/PLA. Therefore, BNC/PLA composites are more thermally stable than neat PLA and CNF/PLA nanocomposite films under 250 °C. However, above 330 °C the CNF/PLA are more thermally stable than BNC/PLA nanocomposites.

Neat PLA has a 0.34% char residue at 400 °C. If each char residue wt% at 400 °C is subtracted by 0.34%, the value is similar to the wt% of the nanocellulose added to the sample. For example, 0.5 wt% BNC/PLA had 0.80% char residue at 400 °C (0.80% minus 0.34% is 0.46%). This is similar to the 0.5 wt% of BNC added during processing of the films. In general, nanocellulose degrades at 335 °C (Dufresne *et al.* 2017). There was some nanocellulose embedded in the PLA fragments that may not have degraded at 400 °C.

Table 4. TGA Data for Neat PLA, CNF/PLA, and BNC/PLA Nanocomposites Films

Samples	$T_{5\%}$ (°C)	$T_{50\%}$ (°C)	Char Residue at 400 °C (%)
Neat PLA	140 ± 1.5	349 ± 3.5	0.34
0.5% CNF/PLA	134 ± 5.0	345 ± 7.5	0.95
1% CNF/PLA	293 ± 1.5	349 ± 0.5	1.26
2% CNF/PLA	296 ± 2.0	350 ± 1.0	1.64
0.5% BNC/PLA	267 ± 34.5	317 ± 25.0	0.80
1% BNC/PLA	265 ± 16.5	315 ± 8.5	0.75
2% BNC/PLA	242 ± 3.0	295 ± 5.0	2.68

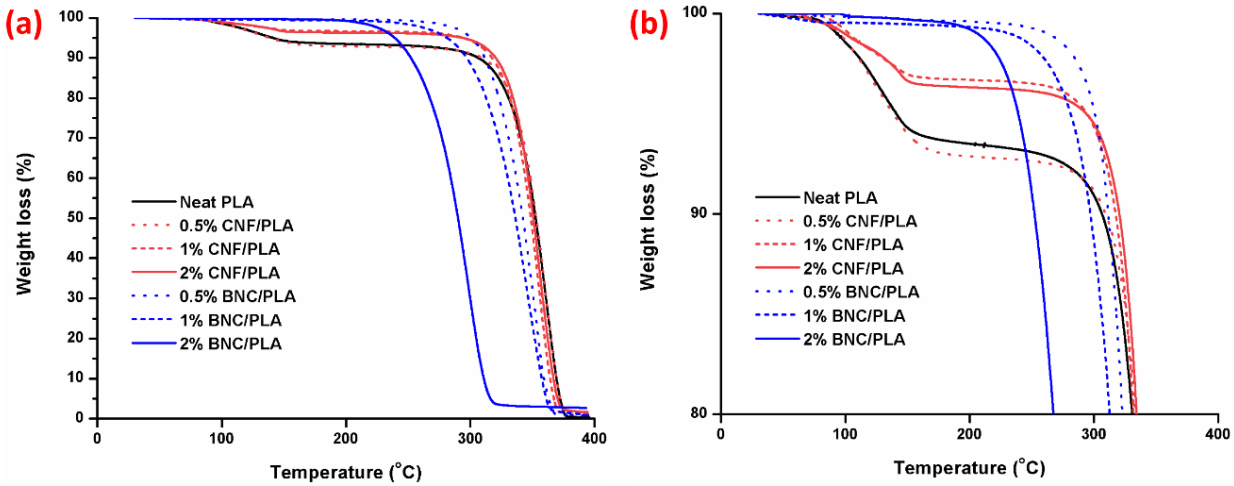

Fig. 8. (a) Thermal gravimetric analysis curves of neat PLA (solid black line), 0.5 wt%, 1.0 wt%, and 2.0 wt% of CNF (red lines) and 0.5 wt%, 1.0 wt%, and 2.0 wt% of BNC (blue lines) and (b) TGA curves comparison for neat PLA and its nanocomposites after at 20% degradation

CONCLUSIONS

1. The bacterial nanocellulose/polylactic acid (BNC/PLA) nanocomposites exhibited higher mechanical properties, *i.e.*, tensile strength and Young's modulus as compared to the default cellulose CNF/PLA and neat PLA without decreasing its toughness at optimum nanocellulose content.
2. Sodium carbonate (Na_2CO_3) was formed *in-situ* on the surface of BNC during fiber purification. The presence of Na_2CO_3 could prevent the agglomeration of BNC by reducing hydrogen bonding between BNC and yield better mechanical performance.
3. The incorporation of BNC induced the growth of imperfect crystal structure in the PLA film and increased the overall degree of crystallinity. 0.5 wt% BNC/PLA had greater overall crystallinity than 0.5 wt% CNF/PLA and neat PLA.
4. The water vapor transmission rate (WVTR) of 0.5 and 1.0 wt% BNC/PLA was lower than the neat PLA and CNF/PLA nanocomposite films which is desirable for food packaging application.
5. BNC/PLA films were more thermally stable than neat PLA and CNF/PLA films below 250 °C. Above 330 °C, CNF/PLA exhibited better thermal stability than BNC/PLA.

ACKNOWLEDGMENTS

The authors are thankful to the Natural Sciences and Engineering Research Council (NSERC), Canada Discovery Grants (Project No. 400320 and 401111); the Ontario Ministry of Agriculture Food and Rural Affairs (OMAFRA), Canada/University of Guelph Bioeconomy-Industrial Uses Research Theme (Project No. 030255); and the Ontario Research Fund, Research Excellence Program, Round-7 (ORF-RE07) from the Ontario Ministry of Research, Innovation, and Science (MRIS), Canada (Project No. 052849 and 052850) for their financial support to carry out this research.

Declaration of interest: none.

REFERENCES CITED

Amin, M. C. I. M., Abadi, A. G., and Katas, H. (2014). "Purification, characterization and comparative studies of spray-dried bacterial cellulose microparticles," *Carbohydr. Polym*. 99, 180-189. DOI: 10.1016/j.carbpol.2013.08.041

Abdulkhani, A., Hosseinzadeh, J., Ashori, A., Dadashi, S., and Takzare, Z. (2014). "Preparation and characterization of modified cellulose nanofibers reinforced polylactic acid nanocomposite," *Polym. Test.* 35, 73-79. DOI: 10.1016/j.polymertesting.2014.03.002

Auad, M. L., Contos, V. S., Nutt, S., Aranguren, M. I., and Marcovich, N. E. (2008). "Characterization of nanocellulose-reinforced shape memory polyurethanes," *Polym. Int.* 57(4), 651-659. DOI: 10.1002/pi.2394

Aulin, C., Salazar-Alvarez, G., and Lindström, T. (2012). "High strength, flexible and transparent nanofibrillated cellulose–nanoclay biohybrid films with tunable oxygen and water vapor permeability," *Nanoscale* 4(20), 6622-6628. DOI: 10.1039/c2nr31726e

Auras, R. A., Harte, B., Selke, S., and Hernandez, R. (2003). "Mechanical, physical, and barrier properties of poly (lactide) films," *J. Plast. Film Sheet.* 19(2), 123-135. DOI: 10.1177/8756087903039702

Blaker, J. J., Lee, K.-Y., and Bismarck, A. (2011). "Hierarchical composites made entirely from renewable resources," *J. Biobased Mater.* Bioenergy 5(1), 1-16. DOI: 10.1166/jbmb.2011.1113

Bowley, S. (2015). "Chapter 4: Variance analysis - Gaussian," in: *A Hitchhiker's Guide to Statistics in Biology*, Any Old Subject Books, Kincardine, ON, Canada, pp. 45-58.

Chen, W., Yu, H., Liu, Y., Hai, Y., Zhang, M., and Chen, P. (2011). "Isolation and characterization of cellulose nanofibers from four plant cellulose fibers using a chemical-ultrasonic process," *Cellulose* 18(2), 433-442. DOI: 10.1007/s10570-011-9497-z

Cox, H. (1952). "The elasticity and strength of paper and other fibrous materials," *Brit. J. Appl. Phys.* 3(3), 72-79. DOI: 10.1088/0508-3443/3/3/302

da Gama, F. M. P. and Dourado, F. (2018) "Bacterial nanocellulose: What future?," *BioImpacts* 8(1), 1-3. DOI: 10.15171/bi.2018.01

Dahlbo, H., Poliakova, V., Mylläri, V., Sahimaa, O., and Anderson, R. (2018). "Recycling potential of post-consumer plastic packaging waste in Finland," *Waste Manage.* 71, 52-61. DOI: 10.1016/j.wasman.2017.10.033

Dollase, W. (1986). "Correction of intensities for preferred orientation in powder diffractometry: application of the March model." *J. Appl. Crystallogr*. 19(4), 267-272. DOI: 10.1107/S0021889886089458

Datta, R., and Henry, M. (2006). "Lactic acid: Recent advances in products, processes and technologies—A review," *J. Chem. Technol. Biot.* 81(7), 1119-1129. DOI: 10.1002/jctb.1486

Fortunati, E., Armentano, I., Zhou, Q., Iannoni, A., Saino, E., Visai, L., Berglund, L. A., and Kenny, J. (2012). "Multifunctional bionanocomposite films of poly (lactic acid), cellulose nanocrystals and silver nanoparticles." *Carbohydr. Polym.* 87(2), 1596-1605. DOI: 10.1016/j.carbpol.2011.09.066

Gacitua, W., Ballerini, A., and Zhang, J. (2005). "Polymer nanocomposites: Synthetic and natural fillers a review," *Maderas-Cienc. Tecnol.* 7(3), 159-178. DOI: 10.4067/S0718-221X2005000300002

Gallegos, A. M. A., Carrera, S. H., Parra, R., Keshavarz, T., and Iqbal, H. M. (2016). "Bacterial cellulose: A sustainable source to develop value-added products – A review," *BioResources* 11(2), 5641-5655. DOI: 10.15376/biores.11.2.

Gea, S. (2010). "Innovative bio-nano composites based on bacterial cellulose," (2010). PhD Thesis, Queen Mary Univ. of London, School of Engineering and Material Sci.

Ghalia, M. A. and Dahman, Y. (2017). "Fabrication and enhanced mechanical properties of porous PLA/PEG copolymer reinforced with bacterial cellulose nanofibers for soft tissue engineering applications," *Polym. Test.* 61, 114-131. DOI: 10.1016/j.polymertesting.2017.05.016

Haafiz, M. M., Hassan, A., Zakaria, Z., Inuwa, I. M., Islam, M. S., and Jawaid, M. (2013). "Properties of polylactic acid composites reinforced with oil palm biomass microcrystalline cellulose," *Carbohydr. Polym.* 98(1), 139-145. DOI: 10.1016/j.carbpol.2013.05.069

He, M., Cho, B.-U., and Won, J. M. (2016). "Effect of precipitated calcium carbonate—Cellulose nanofibrils composite filler on paper properties," *Carbohyd. Polym.* 136, 820-825. DOI: 10.1016/j.carbpol.2015.09.069

Hestrin, S., Aschner, M., and Mager, J. (1947). "Synthesis of cellulose by resting cells of *Acetobacter xylinum*," *Nature* 159, 64-65. DOI: 10.1038/159064a0

Hubbe, M. A., Ferrer, A., Tyagi, P., Yin, Y., Salas, C., Pal, L., and Rojas, O. J., (2017) "Nanocellulose in thin films, coatings, and plies for packaging applications: A review," *BioResources* 12(1), 2143-2233. DOI: 10.15376/biores.12.1.2143-2233

Huda, M., Drzal, L., Mohanty, A., and Misra, M. (2007). "The effect of silane treated- and untreated-talc on the mechanical and physico-mechanical properties of poly(lactic acid)/newspaper fibers/talc hybrid composites," *Compos. Part B-Engineering* 38(3), 367-379. DOI: 10.1016/j.compositesb.2006.06.010

Jonoobi, M., Harun, J., Mathew, A. P., and Oksman, K. (2010). "Mechanical properties of cellulose nanofiber (CNF) reinforced polylactic acid (PLA) prepared by twin screw extrusion," *Compos. Sci. Technol.* 70(12), 1742-1747. DOI: 10.1016/j.compscitech.2010.07.005

Jonoobi, M., Mathew, A.P., Abdi, M.M., Makinejad, M.D., Oksman, K. (2012). "A comparison of modified and unmodified cellulose nanofiber reinforced polylactic acid (PLA) prepared by twin screw extrusion," *J. Polym. Environ.* 20(4), 991-997. DOI: /10.1007/s10924-012-0503-9

Jozala, A. F., de Lencastre-Novaes, L. C., Lopes, A. M., de Carvalho Santos-Ebinuma, V., Mazzola, P. G., Pessoa-Jr, A., Grotto, D., Gerenutti, M., and Chaud, M. V. (2016).

"Bacterial nanocellulose production and application: A 10-year overview," *Appl. Microbiol. Biotechnol.* 100(5), 2063-2072. DOI: 10.1007/s00253-015-7243-4

Kasuga, T., Maeda, H., Kato, K., Nogami, M., Hata, K.-i., and Ueda, M. (2003). "Preparation of poly(lactic acid) composites containing calcium carbonate (vaterite)," *Biomaterials* 24(19), 3247-3253. DOI: 10.1016/S0142-9612(03)00190-X

Krenchel, H. (1964). *Fibre Reinforcement; Theoretical and Practical Investigations of the Elasticity and Strength of Fibre-reinforced Materials*, Doctor's Thesis, University of Copenhagen, København, Denmark.

Lee, K.-Y., Blaker, J. J., and Bismarck, A. (2009a). "Surface functionalisation of bacterial cellulose as the route to produce green polylactide nanocomposites with improved properties," *Compos. Sci. Technol.* 69(15-16), 2724-2733. DOI: 10.1016/j.compscitech.2009.08.016

Lee, S.-Y., Mohan, D. J., Kang, I.-A., Doh, G.-H., Lee, S., and Han, S. O. (2009b). "Nanocellulose reinforced PVA composite films: Effects of acid treatment and filler loading," *Fiber. Polym.* 10(1), 77-82. DOI: 10.1007/s12221-009-0077-x

Lee, K.-Y., Tang, M., Williams, C. K., and Bismarck, A. (2012). "Carbohydrate derived copoly(lactide) as the compatibilizer for bacterial cellulose reinforced polylactide nanocomposites," *Compos. Sci. Technol.* 72(14), 1646-1650. DOI: 10.1016/j.compscitech.2012.07.003

Lee, K.-Y., Aitomaki Y., Berglund, L. A., Oksman, K., and Bismarck, A. (2014). "On the use of nanocellulose as reinforcement in polymer matrix composites." *Compos. Sci. Technol.* 105, 15-27. DOI: 10.1016/j.compscitech.2014.08.032

Li, Z. Q., Zhou, X. D., and Pei, C. H. (2010). "Preparation and characterization of bacterial cellulose/polylactide nanocomposites,"*Polym-Plast. Technol.* 49(2), 141-146. DOI: 10.1080/03602550903284198

Liu, X., Khor, S., Petinakis, E., Yu, L., Simon, G., Dean, K., and Bateman, S. (2010). "Effects of hydrophilic fillers on the thermal degradation of poly (lactic acid)." *Thermochim. Acta* 509(1-2), 147-151. DOI: 10.1016/j.tca.2010.06.015

Luo, X., and Wang, X., (2017). "Preparation and characterization of nanocellulose fibers from NaOH/Urea pretreatment of oil palm fibers," *BioResources* 12(3), 5826-5837. DOI: 10.15376/biores.12.3.5826-5837

Ma, P., Spoelstra, A., Schmit, P., and Lemstra, P. (2013). "Toughening of poly (lactic acid) by poly (*β*-hydroxybutyrate-co-*β*-hydroxyvalerate) with high *β*-hydroxyvalerate content," *Eur. Polym. J.* 49(6), 1523-1531. DOI: 10.1016/j.eurpolymj.2013.01.016

Mathew, A. P., Oksman, K., and Sain, M. (2006). "The effect of morphology and chemical characteristics of cellulose reinforcements on the crystallinity of polylactic acid," *J. Appl. Poly. Sci.* 101(1), 300-310. DOI: 10.1002/app.23346

McLean, E. (1982). "Soil pH and lime requirement," in: *Methods Soil Analysis Part 2 Chemical and Microbiological Properties*, A. L. Page (ed.), American Society of Agronomy, Soil Science Society of America, Madison, WI, pp. 199-224.

Mohammadkazemi, F. (2017) "Surface properties of bacterial nanocellulose using spectroscopic methods and X-ray diffraction," *American Journal of Applied and Industrial Chemistry* 1(1), 10-13. DOI: 10.11648/j.ajaic.20170101.13

Moharram, M. A. and Mahmoud, O. M. (2008). "FTIR spectroscopic study of the effect of microwave heating on the transformation of cellulose I into cellulose II during mercerization," *J. Appl. Poly. Sci.* 107(1), 30-36. DOI: 10.1002/app.26748

Mustapa, I. R., and Shanks, R. A. (2014). "Multiple melting behavior of poly(lactic acid)-hemp-silica composites using modulated-temperature differential scanning

calorimetry," *J. Polym. Eng.* 34(9), 895-903. DOI: 10.1515/polyeng-2013-0161

Nakagaito, A. N., Fujimura, A., Sakai, T., Hama, Y., and Yano, H. (2009). "Production of microfibrillated cellulose (MFC)-reinforced polylactic acid (PLA) nanocomposites from sheets obtained by a papermaking-like process," *Compos. Sci. Technol.* 69(7-8), 1293-1297. DOI: 10.1016/j.compscitech.2009.03.004

Nam, J. Y., Sinha Ray, S., and Okamoto, M., (2003). "Crystallization behavior and morphology of biodegradable polylactide/layered silicate nanocomposite," *Macromolecules* 36(19), 7126-7131. DOI: 10.1021/ma034623j

Panaitescu, D. M., Frone, A. N., Chiulan, I., Gabor, R. A., Spataru, I. C., and Căşărică, A., (2017). "Biocomposites from polylactic acid and bacterial cellulose nanofibers obtained by mechanical treatment," *BioResources* 12(1), 662-672, DOI: 10.15376/biores.12.1.662-672

Park, S., Baker, J. O., Himmel, M. E., Parilla, P. A., and Johnson, D. K. (2010). "Cellulose crystallinity index: Measurement techniques and their impact on interpreting cellulase performance," *Biotechnol. Biofuels* 3(10), 1-10. DOI: 10.1186/1754-6834-3-10

Pei, A., Zhou, Q., and Berglund, L. A. (2010). "Functionalized cellulose nanocrystals as biobased nucleation agents in poly(L-lactide) (PLLA) – Crystallization and mechanical property effects," *Compos. Sci. Technol.* 70(5), 815-821. DOI: 10.1016/j.compscitech.2010.01.018

Petinakis, E., Liu, X., Yu, L., Way, C., Sangwan, P., Dean, K., Bateman, S., Edward, G. (2010). "Biodegradation and thermal decomposition of poly (lactic acid)-based materials reinforced by hydrophilic fillers," *Polym. Degrad. Stab.* 95(9), 1704-1707. DOI: 10.1016/j.polymdegradstab.2010.05.027

PlasticsEurope, E. (2013). Plastics-the Facts 2013. "An analysis of European latest plastics production, demand and waste data," https://www.plasticseurope.org/application/files/7815/1689/9295/2013plastics_the_facts_PubOct2013.pdf

Poyraz, B. (2018). "Enzyme treated CNF biofilms: Characterization," *Int. J. Biol. Macromol.* 117, 713-720. DOI: 10.1016/j.ijbiomac.2018.05.222

Puiggali, J., Ikada, Y., Tsuji, H., Cartier, L., Okihara, T., and Lotz, B. (2000). "The frustrated structure of poly(L-lactide)," *Polymer* 41(25), 8921-8930. DOI: 10.1016/S0032-3861(00)00235-4

Quero, F., Eichhorn, S. J., Nogi, M., Yano, H., Lee, K.-Y., and Bismarck, A. (2012). "Interfaces in cross-linked and grafted bacterial cellulose/poly(lactic acid) resin composites," *J. Polym. Environ.* 20(4), 916-925. DOI: 10.1007/s10924-012-0487-5

Quero, F., Nogi, M., Yano, H., Abdulsalami, K., Holmes, S. M., Sakakini, B. H., and Eichhorn, S. J. (2009). "Optimization of the mechanical performance of bacterial cellulose/poly(L-lactic) acid composites," *ACS Appl. Mater. Inter.* 2(1), 321-330. DOI: 10.1021/am900817f

Reading, M., Luget, A., and Wilson, R. (1994). "Modulated differential scanning calorimetry," *Thermochim. Acta* 238, 295-307. DOI: 10.1016/S0040-6031(94)85215-4

Rhim, J.W., Mohanty, A.K., Singh, S.P., Ng, P.K. (2006). "Effect of the processing methods on the performance of polylactide films: Thermocompression versus solvent casting," *J. Appl. Polym. Sci.* 101(6) , 3736-3742. DOI: 10.1002/app.23403

Salame, M. (1986). "Prediction of gas barrier properties of high polymers," *Polym. Eng. & Science* 26, 1543-1546. doi.org/10.1002/pen.760262203

Segal, L., Creely, J., Martin Jr, A., and Conrad, C. (1959). "An empirical method for estimating the degree of crystallinity of native cellulose using the X-ray

diffractometer," *Text. Res. J.* 29(10), 786-794. DOI: 10.1177/004051755902901003

Shi, Q., Mou, H., Gao, L., Yang, J., and Guo, W. (2010). "Double-melting behavior of bamboo fiber/talc/poly (lactic acid) composites," *J. Polym. Environ.* 18, 567-575. DOI: 10.1007/s10924-010-0252-6

Shi, X., Zhang, G., Phuong, T. V., and Lazzeri, A. (2015). "Synergistic effects of nucleating agents and plasticizers on the crystallization behavior of poly(lactic acid)," *Molecules* 20(1), 1579-1593. DOI: 10.3390/molecules20011579

Shih, Y.-F., and Huang, C.-C. (2011). "Polylactic acid (PLA)/banana fiber (BF) biodegradable green composites," *J. Polym. Res.* 18(6), 2335-2340. DOI: 10.1007/s10965-011-9646-y

Su, Z., Li, Q., Liu, Y., Hu, G. H., and Wu, C. (2009). "Multiple melting behavior of poly(lactic acid) filled with modified carbon black," *J. Polym. Sci. Pol. Phys.* 47(20), 1971-1980. DOI: 10.1002/polb.21790

Tee, Y. B., Talib, R. A., Abdan, K., Chin, N. L., Basha, R. K., and Yunos, K. F. M. (2013). "Thermally grafting aminosilane onto kenaf-derived cellulose and its influence on the thermal properties of poly(lactic acid) composites," *BioResources* 8(3), 4468-4483. DOI: 10.15376/biores.8.3.4468-4483

Ten, E., Jiang, L., and Wolcott, M. P., (2012). "Crystallization kinetics of poly(3-hydroxybutyrate-*co*-3-hydroxyvalerate)/cellulose nanowhiskers composites," *Carbohyd. Polym*. 90(1), 541-550. DOI: 10.1016/j.carbpol.2012.05.076

Tomé, L. C., Pinto, R. J., Trovatti, E., Freire, C. S., Silvestre, A. J., Neto, C. P., and Gandini, A. (2011). "Transparent bionanocomposites with improved properties prepared from acetylated bacterial cellulose and poly(lactic acid) through a simple approach," *Green Chem.* 13(2), 419-427. DOI: 10.1039/C0GC00545B

Wang, L., Ma, W., Gross, R. A., and McCarthy, S. P. (1998). "Reactive compatibilization of biodegradable blends of poly(lactic acid) and poly(ε-caprolactone)," *Polym. Degrad. Stabil.* 59(1-3), 161-168. DOI: 10.1016/S0141-3910(97)00196-1

Yang, W., Fortunati, E., Dominici, F., Kenny, J., and Puglia, D. (2015). "Effect of processing conditions and lignin content on thermal, mechanical and degradative behavior of lignin nanoparticles/polylactic (acid) bionanocomposites prepared by melt extrusion and solvent casting," *Eur. Polym. J.* 71, 126-139. DOI: 10.1016/j.eurpolymj.2015.07.051

Yeh, J. T., Tsou, C. H., Huang, C. Y., Chen, K. N., Wu, C. S., and Chai, W. L. (2010). "Compatible and crystallization properties of poly(lactic acid)/poly(butylene adipate-*co*-terephthalate) blends," *J. Appl. Polym. Sci.* 116(2), 680-687. DOI: 10.1002/app.30907

Zhang, L., Tsuzuki, T., and Wang, X. (2015). "Preparation of cellulose nanofiber from softwood pulp by ball milling," *Cellulose* 22(3), 1729-1741. DOI: 10.1007/s10570-015-0582-6

Article submitted: September 24, 2018; Peer review completed: November 30, 2018; Revised version received and accepted: January 4, 2019; Published: January 18, 2019.
DOI: 10.15376/biores.14.1.1867-1889